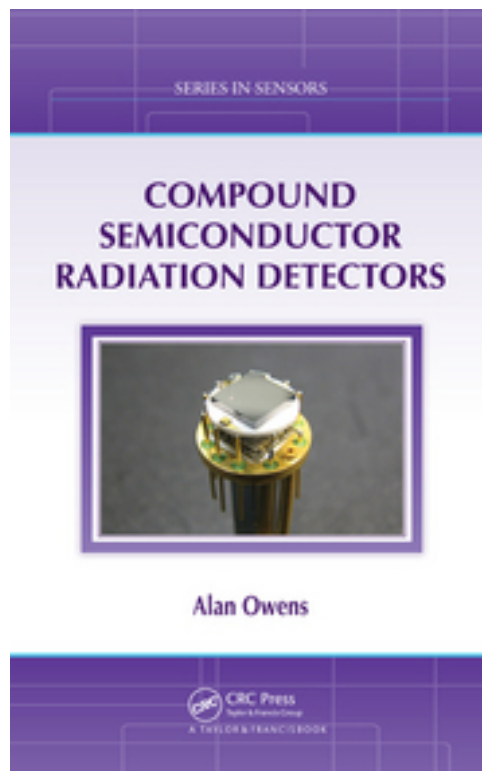


Colour Images from  
*Compound Semiconductor Radiation Detectors*  
Chapter 2

Alan Owens



Bravais Lattice	Primitive (P)	Body Centered (I)	Side Face Centered (C)	All Face Centered (F)	Axes / Interaxial Angles	Examples
Cubic (Isomeric)					$a_1 = a_2 = a_3$ $\alpha_{12} = \alpha_{23} = \alpha_{31} = 90^\circ$	Si, Ge, Au, Zinc Blende structures (e.g., GaAs, InAs, InP, AlSb, CdTe, ZnTe, CZT)
Tetragonal					$a_1 = a_2 \neq a_3$ $\alpha_{12} = \alpha_{23} = \alpha_{31} = 90^\circ$	$\beta$ -Sn, In, HgI <sub>2</sub> , TiO <sub>2</sub> , PbO Chalcopyrite (CuFeS <sub>2</sub> )
Orthorhombic					$a_1 \neq a_2 \neq a_3$ $\alpha_{12} = \alpha_{23} = \alpha_{31} = 90^\circ$	Ga, Cl, I, perovskite (CaTiO <sub>3</sub> ), Bi <sub>2</sub> S <sub>3</sub> , SnS, TIPbI <sub>3</sub>
Hexagonal					$a_1 = a_2 \neq a_3$ $\alpha_{12} = 120^\circ$ $\alpha_{23} = \alpha_{31} = 90^\circ$	Be, Mg, $\beta$ -Quartz, BN, SiC Wurtzite structures (e.g., AlN, $\alpha$ -GaN, InN, ZnO)
Trigonal (R)					$a_1 = a_2 = a_3$ $\alpha_{12} = \alpha_{23} = \alpha_{31} < 120^\circ$	Bi, As, Te, Al <sub>2</sub> O <sub>3</sub> , Bi <sub>2</sub> Te <sub>3</sub> $\alpha$ -Quartz, cinnabar (HgS)
Monoclinic					$a_1 \neq a_2 \neq a_3$ $\alpha_{23} = \alpha_{31} = 90^\circ$ $\alpha_{12} \neq 90^\circ$	Gypsum, As <sub>4</sub> S <sub>4</sub> , KNO <sub>2</sub>
Triclinic					$a_1 \neq a_2 \neq a_3$ $\alpha_{12} \neq \alpha_{23} \neq \alpha_{31}$	B, Cd, Zn, B <sub>4</sub> C, BiI <sub>3</sub> , PbI <sub>2</sub>

Figure 2.1: Schematic of the 7 basic crystal systems and 14 conventional Bravais lattices (for a review see [3]). The lattice centering are: **P** = primitive centering, **I** = body centered, **F** = face centered, **C** = base centered and **R** = rhombohedral (hexagonal class only).

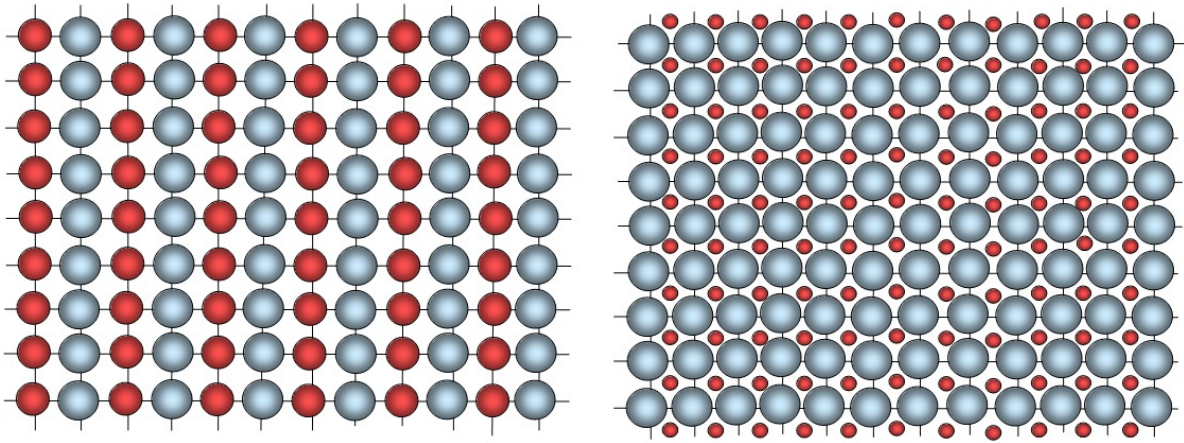


Figure 2.4: (a) schematic of an ordered substitutional cubic lattice in which an atom of one element replaces an atom of the host element in an alternating sequence. The ability to form a stable lattice depends on whether the two species can satisfy the Hume-Rothery rules. (b) example of an interstitial lattice in which the atoms of one element fit interstitially into the spaces in the lattice of the host element.

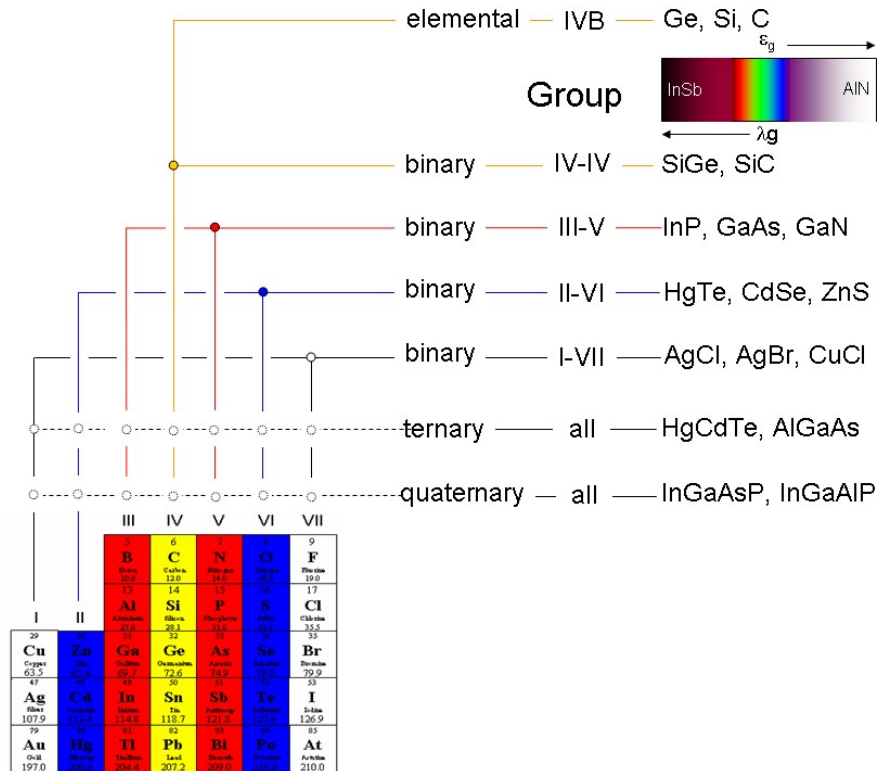


Figure 2.5: Diagram illustrating the relationship of the elemental and compound semiconductors. Examples of the compound type are given and are listed by increasing bandgap energy or alternatively, decreasing wavelength, from the infrared to the ultraviolet. InSb and AlN delineate the extremes of the range in which compound semiconductors lie (0.17 eV – 6.2 eV)

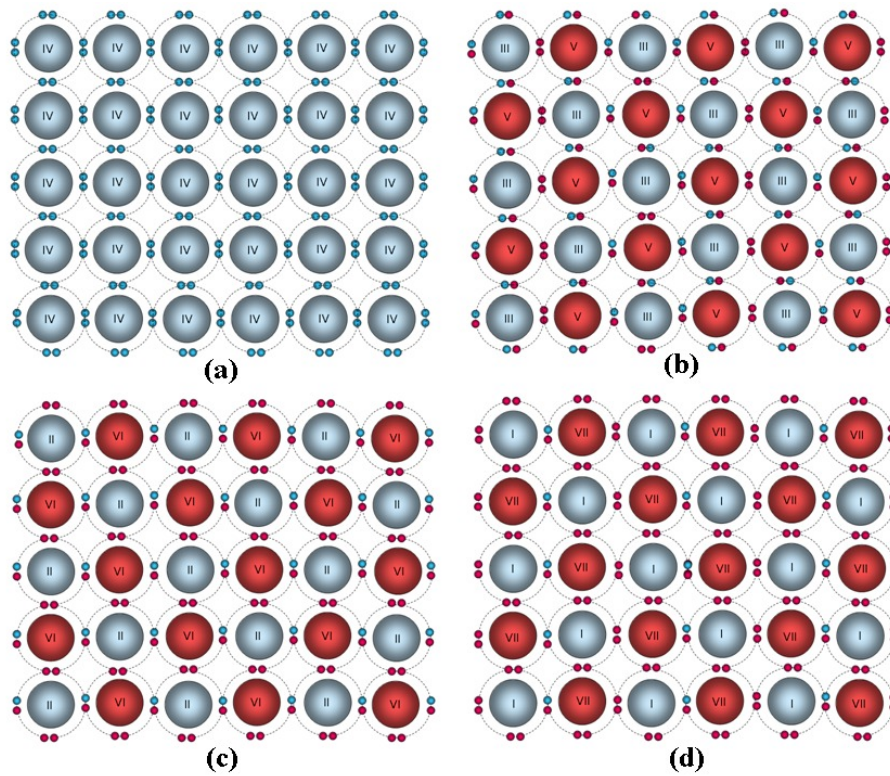


Figure 2.6: Illustration showing how semiconductors bond to form closed valence shells. Examples are given for the four most common semiconductor groups; a) group IV elemental semiconductors, such as Si and Ge b) group III-V semiconductors, such as GaAs and InP, c) group II-VI compounds, such as ZnS and CdTe, and d) group I-VII compounds such as AgCl and AgBr.

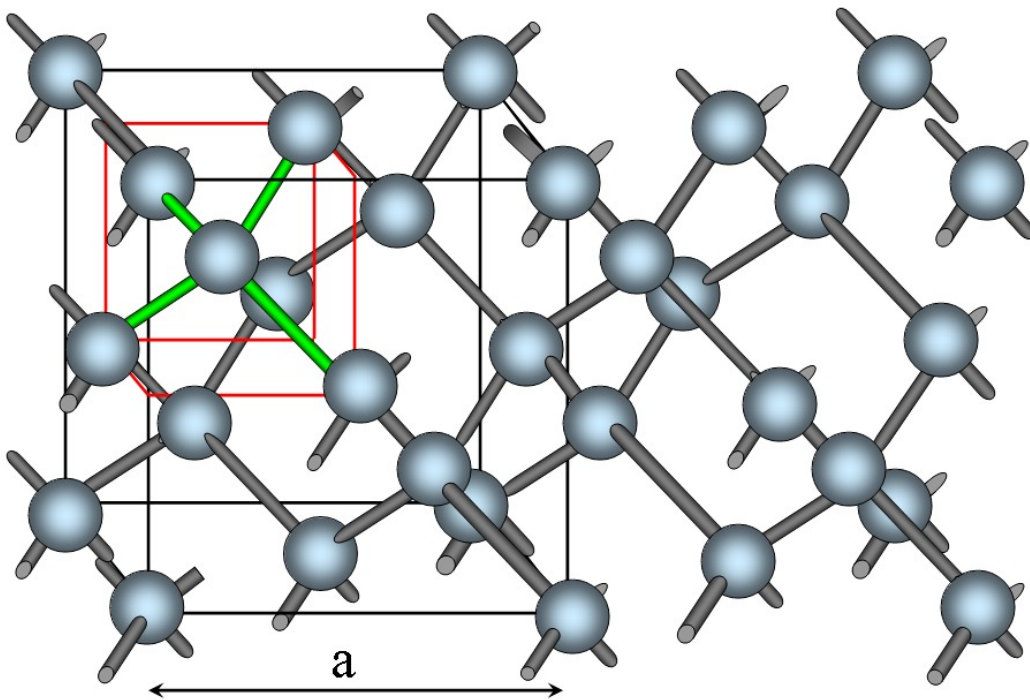


Figure 2.7: The diamond lattice structure. Each atom has four equidistant, tetrahedrally coordinated, nearest neighbours. The unit cell is outlined by the cube of dimension (lattice parameter),  $a$ . The primitive cell containing one lattice point is shown by the green bonds.

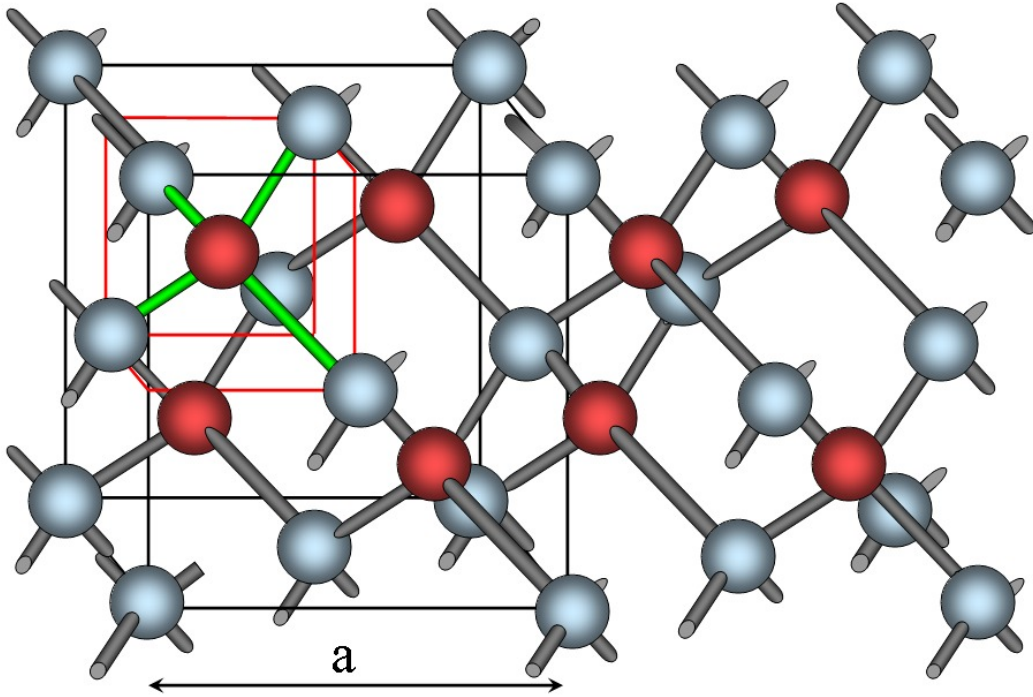


Figure 2.8: The Zinc-Blende lattice structure which is most common structure for binary compound semiconductors. Here, the red and blue spheres denote the atoms of the binary elements. The unit cell is outlined by the cube of dimension (lattice parameter),  $a$ . The primitive cell is shown by the green bonds.

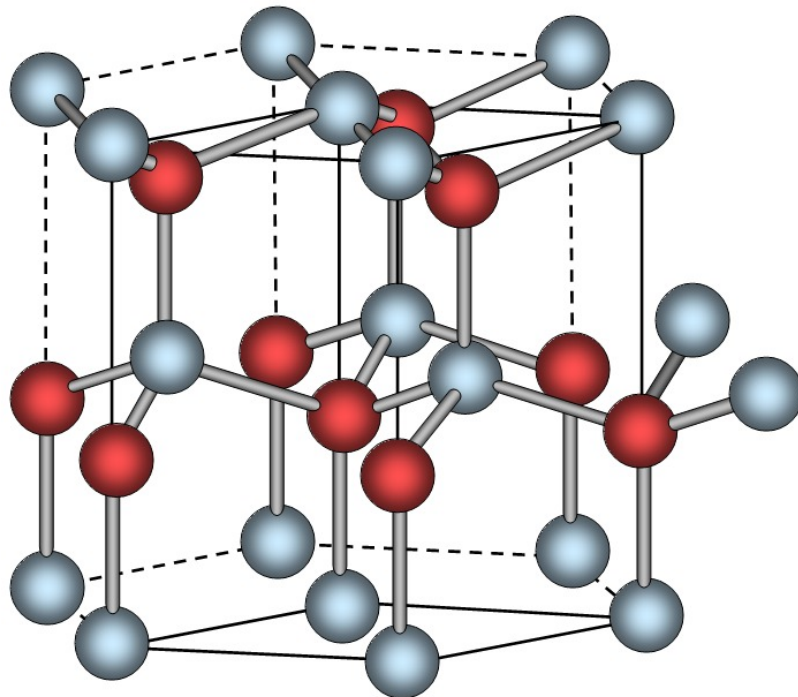


Figure 2.9: The wurtzite lattice structure which is the second most common structure for binary compound semiconductors. Here, the blue and red spheres denote the atoms of individual elements.

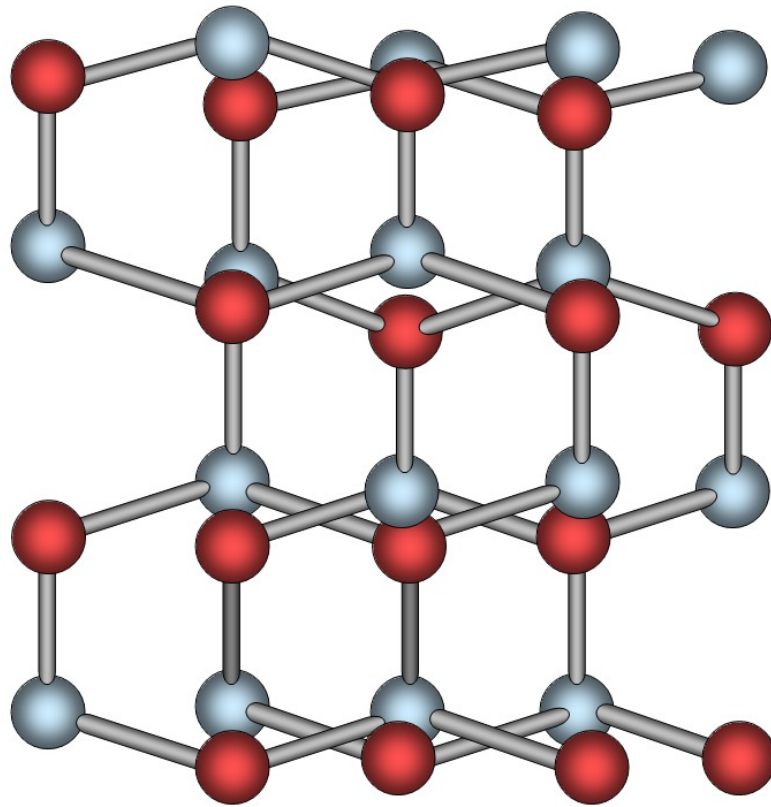


Figure 2.10: A hexagonal lattice structure. The blue and red spheres denote the atoms of individual elements.

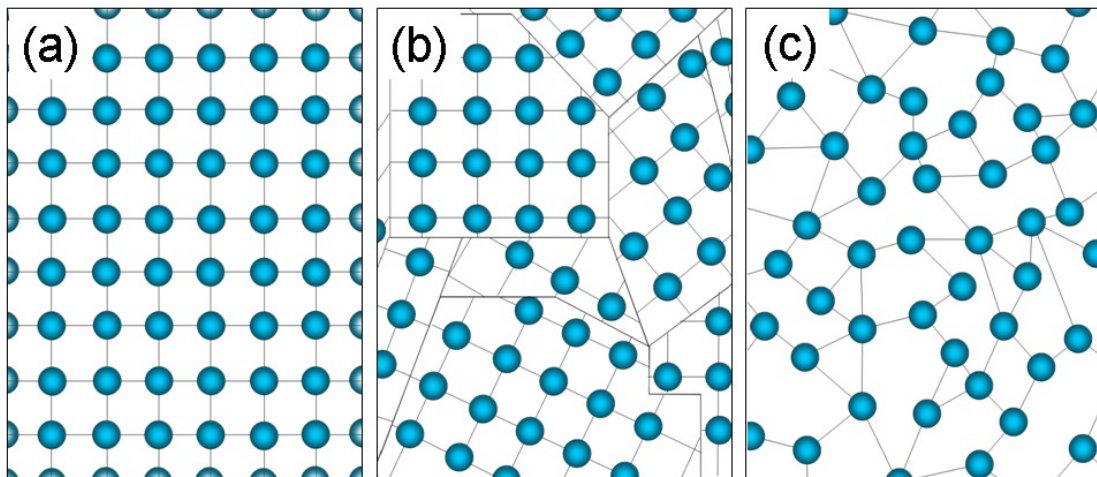


Figure 2.11: Illustration of macroscopic crystal structures in a semiconductor. While the majority of semiconductors solidify into regular periodic patterns (a), they can also form polycrystals, that is, a collection of individual grains of crystalline material separated by grain boundaries or (b) amorphous solid solutions or (c) in which there is little long range order.

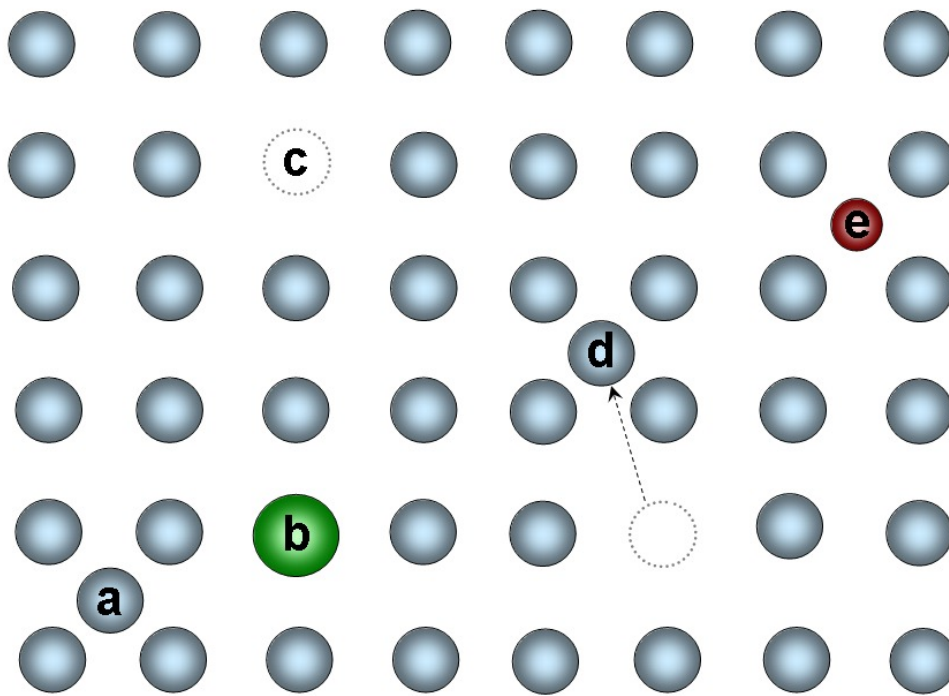


Figure 2.12: Schematic illustrating the different types of point defect in a crystalline material. These are: a) self interstitial atom, b) substitutional impurity atom, c) Schottky defect, d) Frenkel defect, e) interstitial impurity atom.

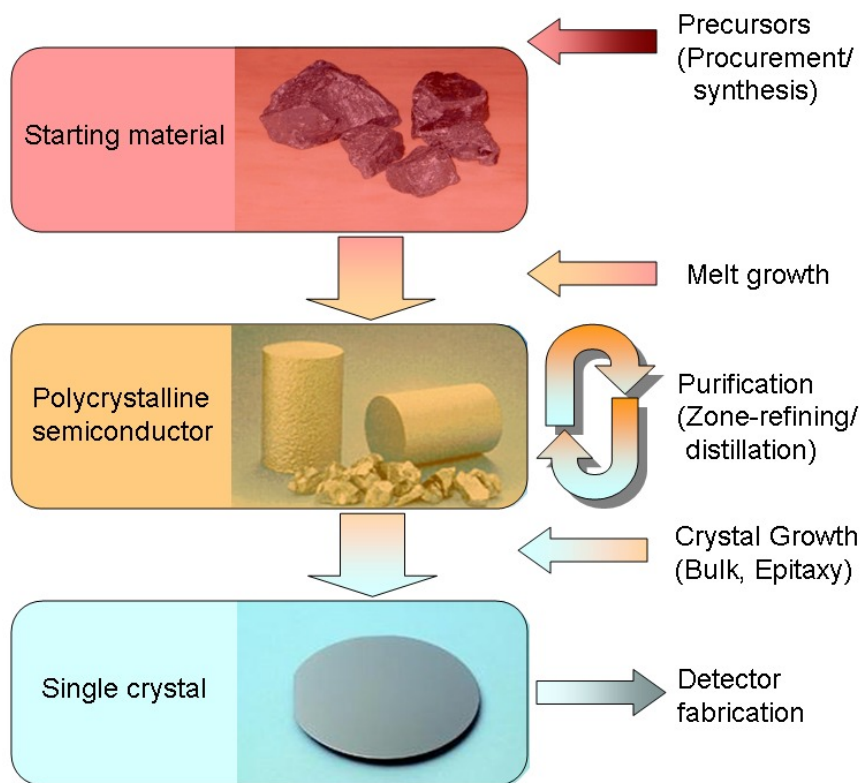


Figure 2.18: Steps required to produce single crystal material for detector production.

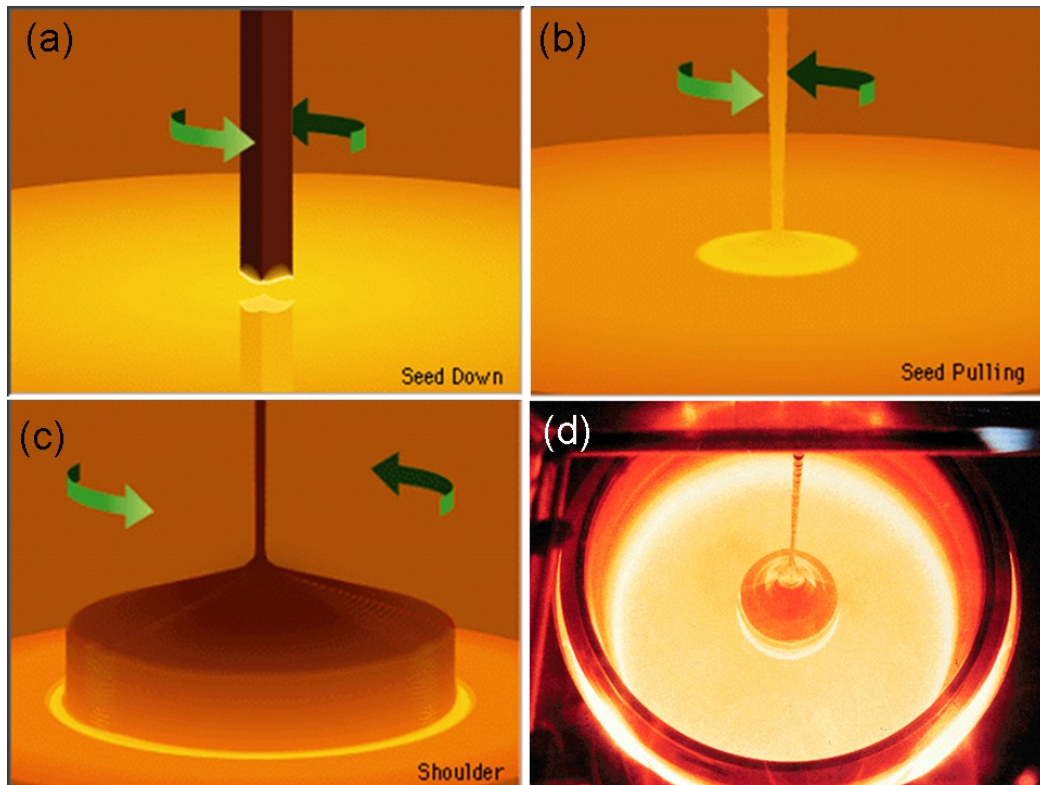


Figure 2.21: Growth sequence in a Czochralski furnace (Images courtesy of Kinetic Systems Inc.). (a) seed crystal is lowered into the melt, (b) as crystallization begins the rod holding the seed crystal is slowly withdrawn, (c) by varying the pull rate the diameter of crystal can be controlled, forming the basis of the ingot, (d) a view into an actual crucible during the drawing of an ingot.

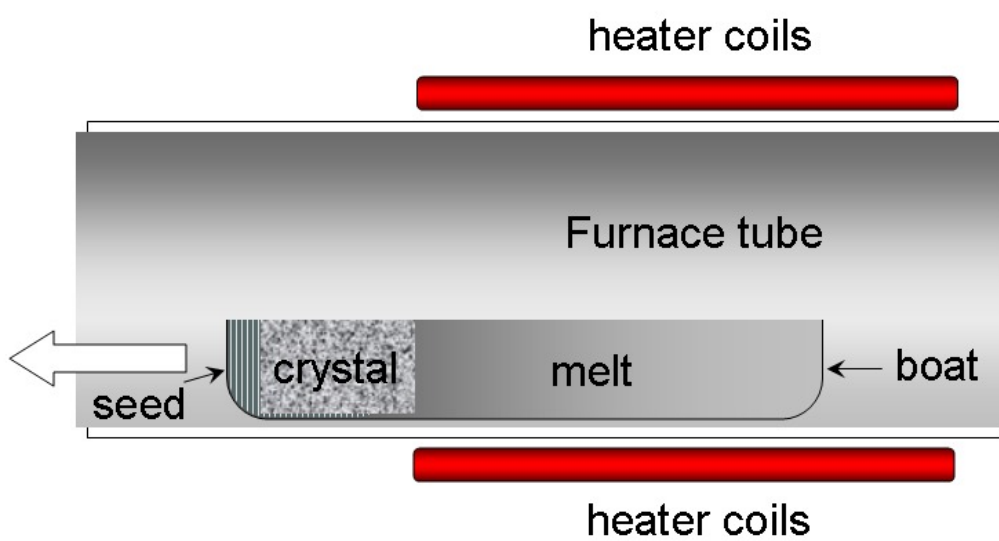


Figure 2.25: Schematic of the horizontal Bridgman method. The crystal is solidified by slowly withdrawing the charge from the heater.

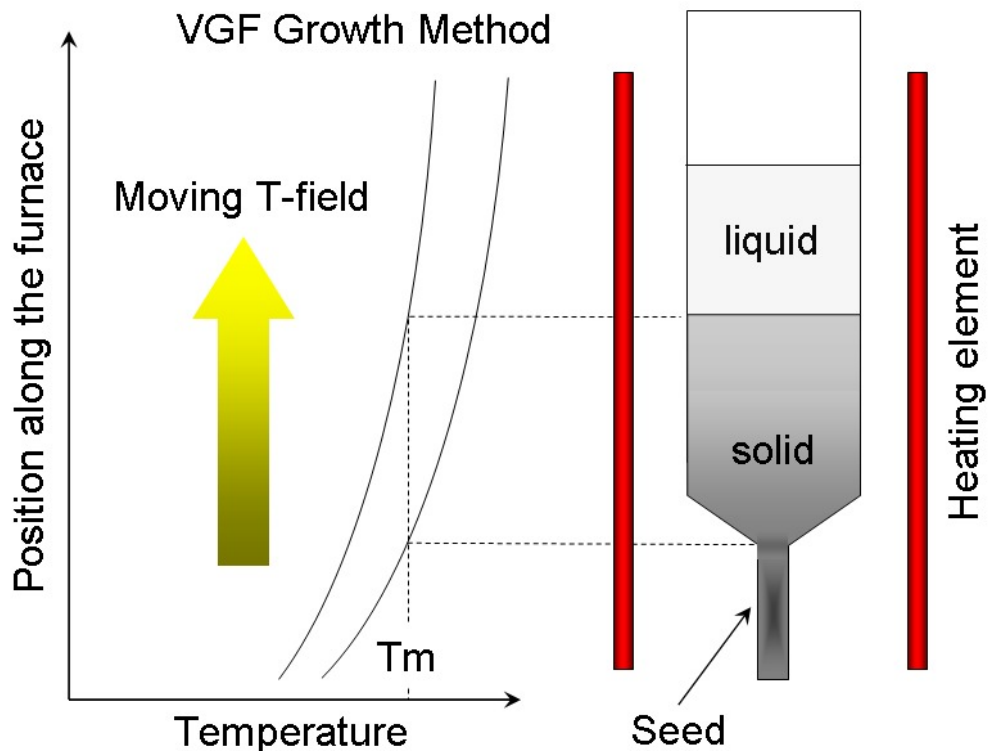


Figure 2.28: Essential elements of the Vertical Freeze Growth (VGF) method. Left: the furnace temperature profile. Right: the material state along the charge.  $T_m$  is the melting temperature.

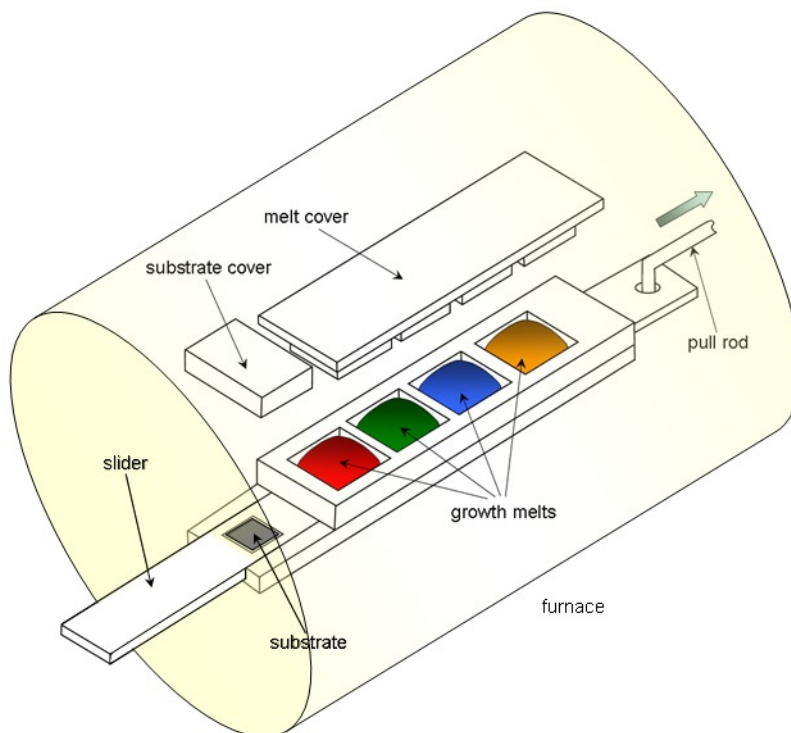


Figure 2.32: A schematic of a LPE growth system suitable for growing heterostructures. The slider can be moved so that it is aligned with the different melts.

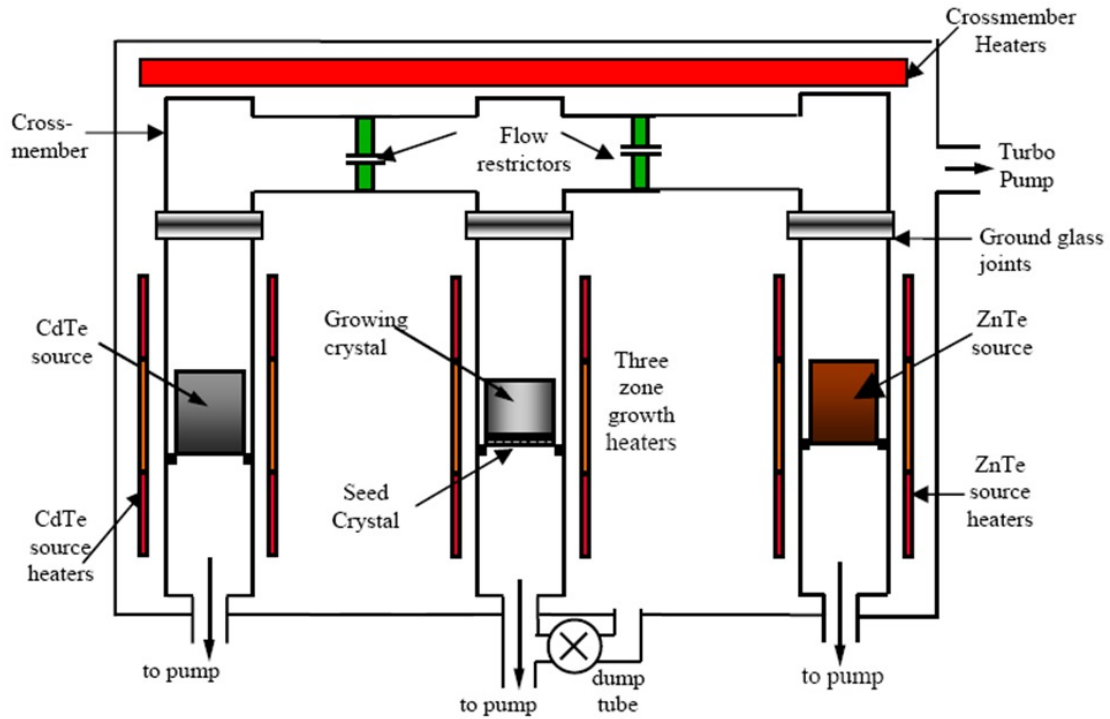


Figure 2.34: Schematic of the essential components of the Multi-Tube Physical Vapour Transport (MTPVT) growth system used to grow CdZnTe (figure courtesy Kromek®).

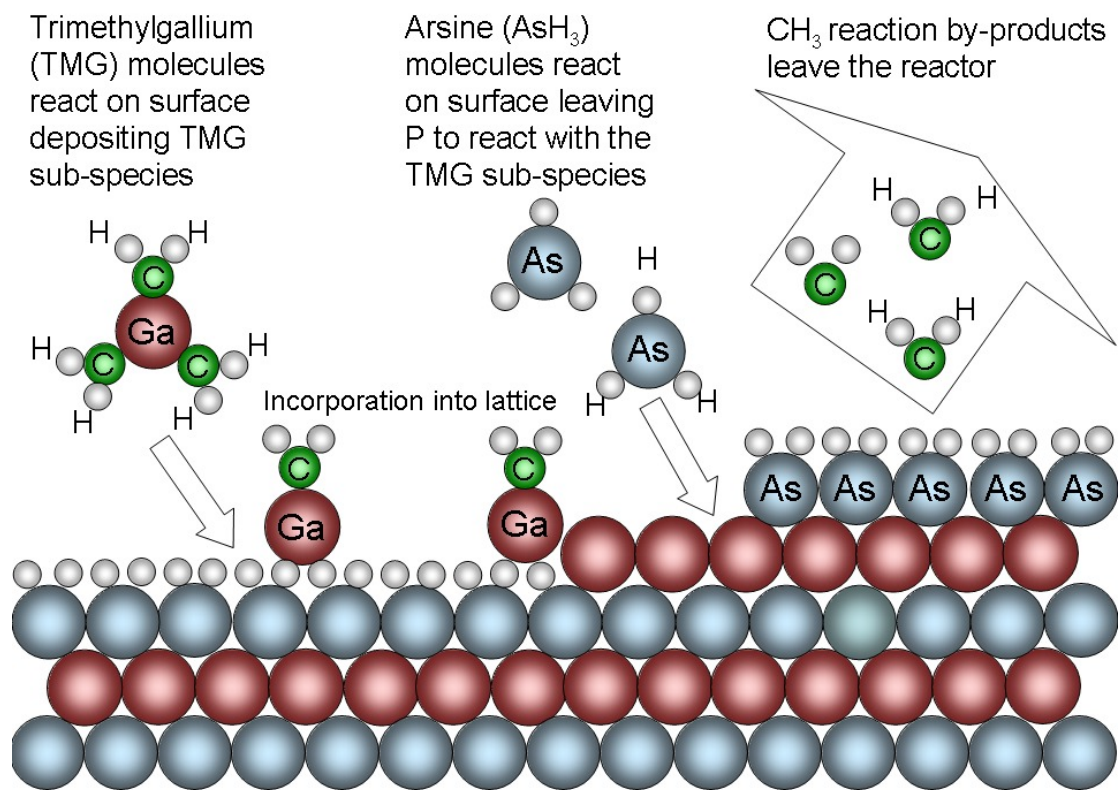


Figure 2.36: Figure illustrating the principle behind the MOCVD growth of GaAs.

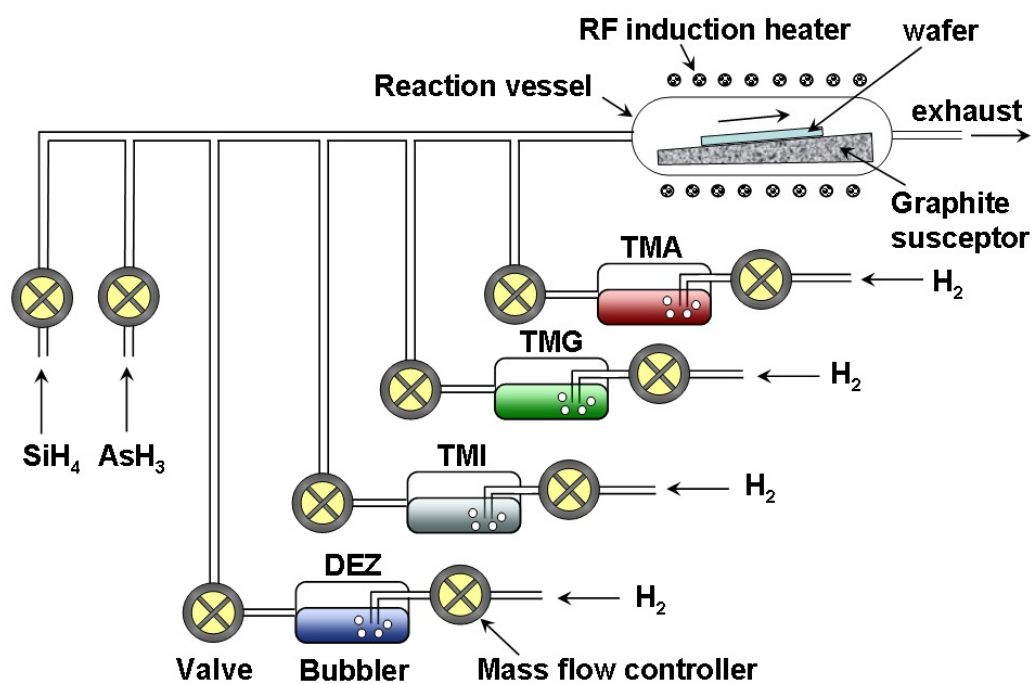


Figure 2.37: Schematic of the essential components of a typical MOCVD reactor system for the growth of a range of III-V compounds (modified from [66]). Here, the organometallic precursors are: TMA = trimethylaluminum, TMG = trimethylgallium, TMI = trimethylindium, DEZ = diethylzinc,  $\text{AsH}_4$  = arsine and  $\text{SiH}_4$  = silane.